



Comparison of MR T1 and T2 mapping parameters to characterize myocardial and skeletal muscle involvement in systemic idiopathic inflammatory myopathy (IIM)

Adrian T. Huber^{1,2,3} · Jérôme Lamy^{1,4} · Marine Bravetti^{1,2} · Khaoula Bouazizi^{1,4} · Tania Bacoyannis¹ · Charles Roux^{1,2} · Alain De Cesare¹ · Aude Rigolet⁵ · Olivier Benveniste^{5,6} · Yves Allenbach^{5,6} · Mathieux Kerneis⁷ · Philippe Cluzel^{1,2,4} · Alban Redheuil^{1,2,4} · Nadjia Kachenoura^{1,4}

Received: 20 September 2018 / Revised: 19 December 2018 / Accepted: 30 January 2019
© European Society of Radiology 2019

Abstract

Objectives To compare the performance of magnetic resonance (MR) relaxometry parameters to discriminate myocardial and skeletal muscle inflammation in idiopathic inflammatory myopathy (IIM) patients from healthy controls.

Materials and methods For this retrospective case-control study, 20 consecutive IIM patients (54 ± 18 years, 11 females) with cardiac involvement (troponin level > 50 ng/l) and 20 healthy controls (47 ± 12 years, 9 females) were included. All patients without cardiac MR imaging < 2 weeks prior to the laboratory testings were excluded. T1/T2 relaxation times, as well as T1-derived extracellular volume (ECV), relative tissue T1 shortening $\Delta T1 = (\text{native } T1_{\text{tissue}} - \text{post contrast } T1_{\text{tissue}}) / \text{native } T1_{\text{tissue}}$, and enhancement fraction EHF $= (\text{native } T1_{\text{tissue}} - \text{post contrast } T1_{\text{tissue}}) / (\text{native } T1_{\text{blood}} - \text{post contrast } T1_{\text{blood}})$, were compared using Mann-Whitney *U* test and ROC analysis.

Results All measured MR relaxometry parameters significantly discriminated IIM patients and healthy controls, except T2 in skeletal muscles and ECV in the myocardium. In skeletal muscles, post contrast T1 and T1-derived parameters showed the best performance to discriminate IIM patients from healthy controls (AUC = 0.98 for post contrast T1 and AUC 0.94–0.97 for T1-derived parameters). Inversely, in the myocardium, native T1 and T2 showed better diagnostic performance (AUC = 0.89) than post contrast T1 (AUC = 0.76), ECV (AUC = 0.58), $\Delta T1$ (AUC = 0.80) and EHF (0.82).

Conclusions MR relaxometry parameters applied to the myocardium and skeletal muscles might be useful to separate IIM patients from healthy controls. However, different tissue composition and vascularization should be taken into account for their interpretation. $\Delta T1$ and EHF may be simple alternatives to ECV in highly vascularized tissues such as the myocardium.

Key Points

- MR relaxometry parameters applied to the myocardium and skeletal muscles are highly useful to separate IIM patients from healthy controls.
- Different tissue composition and vascularization should be taken into account for T1 and T2 mapping parameter interpretation.
- $\Delta T1$ and EHF may be simple alternatives to ECV in highly vascularized tissues such as the myocardium.

Keywords Idiopathic inflammatory myopathy · Myocarditis · Magnetic resonance imaging · Skeletal muscle · Extracellular space

Alban Redheuil and Nadjia Kachenoura contributed equally to this work.

✉ Nadjia Kachenoura
nadjia.kachenoura@inserm.fr

¹ Sorbonne Université, INSERM, CNRS, Laboratoire d'Imagerie Biomédicale, Paris, France

² Department of Cardiovascular and Thoracic Imaging and Interventional Radiology, Institute of Cardiology, Hôpital Pitié-Salpêtrière, Paris, France

³ Department of Diagnostic, Interventional and Pediatric Radiology, Inselspital, Bern University Hospital, University of Bern, Bern, Switzerland

⁴ Institute of Cardiometabolism and Nutrition (ICAN), Paris, France

⁵ Department of Internal Medicine, Hôpital Pitié-Salpêtrière, Paris, France

⁶ Centre de Recherche en Myologie, INSERM UMR974, Sorbonne Université, Paris, France

⁷ Department of Cardiology, Institute of Cardiology, Hôpital Pitié-Salpêtrière, Paris, France

Abbreviations

AVM	Acute viral myocarditis
ECS	Extracellular space
ECV	Extracellular volume
EF	Ejection fraction
EHF	Enhancement fraction
IIM	Idiopathic inflammatory myopathy
MOLLI	Modified Look-Locker inversion recovery
MR	Magnetic resonance
SAPPHIRE	Saturation pulse prepared heart rate independent inversion recovery
SASHA	Saturation recovery single-shot acquisition
TE	Echo times
TI	Times of inversion

Introduction

Due to a paradigm shift from qualitative image interpretation towards the use of quantitative magnetic resonance (MR) imaging, multiparametric and functional biomarkers, such as T1 and T2 parametric mapping techniques, are increasingly used [1]. They allow absolute quantification of T2 and T1 relaxation times in every voxel (native or after contrast agent injection) and are sensitive to fat, edema, inflammation, and fibrosis contents [2]. The modified Look-Locker inversion recovery (MOLLI) sequences have been proposed for T1 quantification, where T1 times are calculated in every pixel using an exponential fit from signal intensities at different times of inversion (TI) after two or more Look-Locker 180° inversion pulses [3]. Other methods, such as saturation recovery single-shot acquisition (SASHA) and saturation pulse prepared heart rate independent inversion recovery (SAPPHIRE), use different technical approaches with shorter acquisition times and higher accuracy than MOLLI but lower precision [4]. For T2 quantification, a T2-prepared bSSFP sequence allows a 3-point exponential fit at different echo times (TE) to quantify T2 relaxation times in every pixel [5].

Gadolinium-based contrast agents distribute in the extracellular space (ECS) of the human body, but spare the intracellular space [6]. While the relaxation rates correlate to the amount of tissue-distributed gadolinium, different tissue types show different relaxation rates during the equilibrium phase [7]. This reflects different proportions of extracellular and intracellular spaces, which can be used to characterize pathologies with ECS expansion (such as fibrosis or inflammation) and cellular damage [8]. Tissue and blood pool native and post contrast T1 relaxation times can be combined to calculate non-invasive imaging biomarkers, such as the extracellular volume (ECV) fraction [9]. The basis for ECV calculation is the assumption that gadolinium is equally distributed in the ECS between the interstitial and vascular compartments [10]. Other parameters based on native and post contrast T1 can

be estimated: (1) $\Delta T1$ which is calculated as the native to post contrast difference in T1 relaxation times normalized by native T1 [11], and (2) the tissue enhancement fraction (EHF) calculated as the tissue to blood pool ratio of native to post contrast T1 differences. While $\Delta T1$ is exclusively a tissue index, ECV and EHF take into account T1 shortening of the blood pool. Both $\Delta T1$ and EHF do not require the patient's hematocrit, but are not frequently reported in the literature, with the exception of some liver imaging studies [11, 12]. In contrast, ECV is widely used in cardiac imaging [13] and has been shown to correlate well with interstitial myocardial fibrosis histological grade in explanted hearts [14]. However, several studies have shown better diagnostic performance of T1 and T2 relaxation times alone, as compared to ECV, for example in myocarditis patients [15], where quantification of T1 and T2 relaxation times (but not ECV) supersedes original Lake-Louise criteria [16, 17].

A special case of myocarditis is autoimmune cardiac inflammation related to idiopathic inflammatory myopathy (IIM) [18], including dermatomyositis, polymyositis, and other subgroups of autoimmune systemic myositis [19]. IIM leads to autoimmune systemic muscular inflammation and is routinely diagnosed by clinical investigation, electromyography, and biopsy of skeletal muscles. A review of scarcely available literature by Gupta et al [18] analyzed 13 pathology articles with 68 patients, showing myocarditis in 19/68 patients and myocardial fibrosis in 21/68 patients, while in 6 articles reporting cardiac symptoms just 15/195 patients were reported to present clinically with angina and 11/195 patients had congestive heart failure.

Since IIM patients show inflammation in both myocardium and skeletal muscles, analyzable in the same cardiac MR field of view, we aimed to use IIM as a model to assess the diagnostic performance of different MR relaxometry parameters in terms of myocardial and skeletal muscle inflammation characterization.

Materials and methods

Population

This retrospective case-control study complied with the Declaration of Helsinki and was approved by the local ethics committee. All participants signed an informed consent. A total of 40 study participants were included in a tertiary referral center between January 2014 and November 2015: 20 consecutive patients with proven IIM based on skeletal muscle biopsies and immunology markers, who underwent cardiac MR imaging because of suspected non-infectious cardiac inflammation, based on elevated cardiac troponin levels > 50 ng/ml, as well as 20 healthy controls with equivalent age, gender, and body size distribution. Excluded were IIM

patients without MR imaging within 2 weeks of laboratory tests and patients with prior cardiac events. IIM subgroups consisted of seven patients with necrotizing autoimmune myopathies, five patients with anti-synthetase syndrome, and eight patients with other IIM subtypes (polymyositis, dermatomyositis, overlap syndrome).

Cardiac MR imaging

All subjects underwent a routine clinical cardiac MR exam on a 1.5 T magnet (Magnetom Aera, Siemens Healthcare) using the following sequences as published before [20]: (1) balanced steady-state free precession (bSSFP) cine imaging in short- and long-axis views with the following parameters: acquisition matrix = 216×256 , repetition time = 51.12 ms, echo time = 1.19 ms, flip angle = 53° , pixel size = $1.48 \times 1.48 \text{ mm}^2$, slice thickness = 6 mm, and inter-slice gap = 1 mm. Temporal resolution was between 10 and 40 ms; (2) short- and long-axis LGE images acquired with a single-shot inversion recovery sequence 10 min after injection of 0.2 mmol/kg of gadobenate dimeglumine (Multihance, Bracco) with the following scan parameters: acquisition matrix = 240×240 , inversion time individually chosen on TI scout, repetition time = 347.21 ms, echo time = 1.18 ms, flip angle = 40° , pixel size = $1.46 \times 1.46 \text{ mm}^2$, slice thickness = 8 mm, and inter-slice gap = 0.8 mm; (3) motion-corrected Look-Locker inversion recovery (MOLLI) T1 mapping sequence with a 5(3)3 scheme before and 15 min after intravenous contrast agent injection with the following parameters: acquisition matrix = 218×256 , echo time = 1.12 ms, repetition time = 344 ms, flip angle = 35° , pixel size = $1.41 \times 1.41 \text{ mm}^2$, and slice thickness = 8 mm; (4) T2 mapping using a 3-point T2-prepared bSSFP sequence before contrast injection with the following scan parameters: acquisition matrix = 206×256 ; echo times = 0, 24, 55 ms; repetition time = 300 ms; flip angle = 35° ; pixel size = $1.41 \times 1.41 \text{ mm}^2$; and slice thickness = 8 mm. Both T1 and T2 mapping acquisitions were performed in basal, mid-LV, and apical short-axis slices. Left ventricular volumes, mass, and ejection fraction (EF) were assessed on short-axis images.

Image post processing

T1 and T2 mapping were analyzed on a custom software as presented before [20]. In skeletal muscles, T1 was calculated using a single exponential fit performed on the mean signal extracted from regions of interest positioned manually on the same muscle for all TI images (A.H., 7 years of experience in cardiac imaging). This was done rather than a pixel-based calculation to minimize the effect of motion and deformation on our estimate. This process was repeated for five skeletal muscle groups (pectoralis major, subscapularis, infraspinatus, brachial, and erector spinae muscles), as visible in the

acquired cardiac field of view. Measured T1/T2 values of the five different skeletal muscle groups were then averaged to get one mean skeletal muscle value for every individual. T1 relaxation times in the myocardium were calculated by assigning exponential fits to each pixel to calculate pixel-wise T1 values and then averaged over the delineated myocardium. To mimic the slice-based calculation performed for the skeletal muscle, myocardial T1 was also calculated by assigning one exponential fit to the signal averaged over all myocardial pixels to calculate a single T1 value for the whole slice. In both cases, whole heart mean T1 values were calculated by averaging basal and mid-LV T1 values. Similar to T1, T2 values were calculated using the pixel-wise approach for the myocardium and the slice-based approach for both myocardium and skeletal muscle. For both myocardium and skeletal muscle ECV, EHF and $\Delta T1$ were calculated as follows:

$$\begin{aligned} \text{ECV} &= (1 - \text{hematocrit}) * \lambda, \text{ with } \lambda \\ &= \frac{\frac{1}{\text{post contrast T1 tissue}} - \frac{1}{\text{native T1 tissue}}}{\frac{1}{\text{post contrast T1 blood pool}} - \frac{1}{\text{native T1 blood pool}}} \end{aligned} \quad (1)$$

Please note that extracellular, intravascular space is neglected in the ECV formula [14].

$$\Delta T1 = \frac{\text{native T1 tissue} - \text{post contrast T1 tissue}}{\text{native T1 tissue}} \quad (2)$$

$$\text{EHF} = \frac{\text{native T1 tissue} - \text{post contrast T1 tissue}}{\text{native T1 blood pool} - \text{post contrast T1 blood pool}} \quad (3)$$

Statistical analysis

The sample size was based on a power analysis using previous [16] T1 mapping results in acute viral myocarditis compared with healthy controls, presuming similar T1 values in acute viral myocarditis and IIM myocarditis. A necessary sample size of 19 patients and 19 controls was calculated with an α -error of 0.05 and a power of 90% to differentiate cardiac inflammation from normal myocardium with native T1. Comparison of IIM patients and controls was done with non-parametric Mann-Whitney test for continuous and Fisher's exact test for categorical variables. Quantitative measures obtained in the IIM subgroups were compared using a Kruskal-Wallis test. ROC analysis was used to obtain the best discriminating parameter in skeletal and myocardial muscles to differentiate IIM patients and controls. Any $p < 0.05$ was regarded as significant. Statistical software package Stata

software (Version 11.2, Stata Corp) and GraphPad Prism (Version 7.1, GraphPad Software Inc) were used.

Results

Patients and imaging baseline characteristics are shown in Table 1. There was no significant difference in hematocrit levels ($p = 0.089$) between the IIM and the control group. IIM patients with cardiac involvement showed reduced creatinine levels, as compared to controls ($p < 0.001$), but elevated troponin T (583 ± 651 ng/ml) and CPK (2438 ± 3547 U/l) (such measures were not available in the control group). The time between diagnosis and cardiac MR imaging was 57 months on average and all IIM patients were under immunosuppressive therapy at the time of cardiac MR imaging. Clinically, 19 patients (95%) presented with muscle weakness, 7 patients (35%) with myalgia, 6 patients with dyspnea (30%), and 2 patients (10%) with dysphagia. There was no significant difference in the left ventricular volumes, mass, and LV EF between the IIM patients and healthy controls. However, while 4 out of 20 patients showed reduced LVEF $< 50\%$, all of the healthy controls by definition had normal LVEF. Thirty-five percent of the IIM patients showed LGE in at least one cardiac segment, but only 5% of all cardiac segments of IIM patients were LGE-positive with an exclusively non-ischemic pattern (18/340 segments, minimum of 1 and maximum of 5 segments per patient, median of 2 segments were LGE-positive). Zero out of 18 LGE-positive segments had a subendocardial localization, while 9/18 were intramural and 9/18 subepicardial. Comparison between IIM subgroups showed no significant differences in terms of clinical parameters, myocardial volumes, and ejection fraction as well as myocardial mapping parameters. However, there was a slightly higher native T1 of the skeletal muscles in patients with anti-synthetase syndrome and higher T2 of the skeletal muscles in patients with polymyositis, dermatomyositis, or overlap syndrome ($p = 0.02$ and $p = 0.04$, respectively).

Mean values of different mapping parameters with standard deviations are shown in Table 2, comparing the two groups with a per slice-based approach as well as on a per pixel-based approach in myocardium. In skeletal muscles, post contrast T1 (sensitivity = 100%, specificity = 85%, accuracy = 93%, and AUC = 0.98) and T1 mapping-derived parameters, especially $\Delta T1$ (sensitivity = 95%, specificity = 95%, accuracy = 95%, and AUC = 0.97), were able to discriminate between IIM patients and controls with high performance, with a slight inferiority for native T1 (sensitivity = 84%, specificity = 75%, accuracy = 79%, and AUC = 0.81). T2 was not helpful in skeletal muscles in terms of IIM and control discrimination. When measured in the myocardium, native T1 (sensitivity = 90%, specificity = 75%, accuracy = 83%, and AUC = 0.89) and T2 (sensitivity = 75%, specificity = 95%, accuracy =

Table 1 Baseline clinical and imaging characteristics of the study population

	Controls ($n = 20$)	IIM ($n = 20$)	p value
Age, years	47 \pm 12	54 \pm 18	0.163
Male/female	11 / 9	9 / 11	
BMI (kg/m^2)	25 \pm 4	22 \pm 3	0.095
Arterial Hypertension	0 (0%)	3 (15%)	0.231
Dyslipidemia	0 (0%)	5 (25%)	0.047
Diabetes	0 (0%)	2 (10%)	0.487
NT-proBNP (pg/ml)	N/A	699 \pm 1226	
Troponin T, (ng/ml)	N/A	583 \pm 651	
CPK (U/l)	N/A	2438 \pm 3547	
Hematocrit (%)	42 \pm 3	40 \pm 3	0.089
Creatinine ($\mu\text{mol}/\text{l}$)	82 \pm 14	50 \pm 20	< 0.001
CRP (mg/l)	1 \pm 1	15 \pm 25	< 0.001
LV EDV index (ml/m^2)	79 \pm 16	78 \pm 15	0.718
LV ESV index (ml/m^2)	32 \pm 6	35 \pm 13	0.942
LV mass index (ml/m^2)	54 \pm 11	55 \pm 14	0.919
LV EF (%)	59 \pm 4	56 \pm 10	0.792
LGE-positive patients	0 (0%)	7 (35%)	0.008
LGE-positive cardiac segments, median (range)	0 (0)	2 (1–5)	< 0.001

Values are mean \pm SD or n . $p < 0.05$ Mann-Whitney U or Fisher's exact test, as appropriate

IIM, idiopathic inflammatory myopathy; BMI, body mass index; NT-proBNP, N-terminal pro b-type natriuretic peptide; CPK, creatinine phosphokinase; CRP, C-reactive protein; LV, left ventricular; EDV, end-diastolic volume; ESV, end-systolic volume; EF, ejection fraction; LGE, late gadolinium enhancement

85%, and AUC = 0.89) were the best discriminators in the per slice-based approach. EHF and $\Delta T1$ showed a slightly lower performance, and ECV and λ were not significantly different between IIM and controls. There was no substantial difference between the per pixel- and the per slice-based approach for myocardial parameters in terms of IIM and controls discrimination as well as in terms of standard deviations of the measurements in both populations. For illustration, T1 and T2 values based on the per slice approach are plotted in Fig. 1 for both myocardium and skeletal muscle. While gadolinium injection leads to more pronounced T1 shortening in the myocardium compared to the skeletal muscle, differences of T1 shortening between IIM patients and controls were higher in the skeletal muscle, as indicated by $\Delta T1$ variation between the two groups in Table 2. Slightly larger confidence intervals were noted in skeletal muscles compared with the myocardium, especially for T2. In the control group, T1/T2 values were quite similar between the five different skeletal muscle groups (pectoralis major, subscapularis, infraspinatus, brachial, and erector spinae muscles) for post contrast T1 (495–527 ms), ECV (9–12%), EHF (23–28%), $\Delta T1$ (37–41%), and T2 (39–

Table 2 CMR mapping parameters

	Controls (n = 20)	IIM (n = 20)	p value	ROC AUC	p value	Cutoff	Sensitivity	Specificity	Accuracy
Skeletal muscles per slice-based approach									
T1 native (ms)	842 ± 39	964 ± 127	< 0.001	0.81	0.001	860	84	75	79
T1 contrast, 15 min (ms)	512 ± 47	374 ± 55	< 0.001	0.98	< 0.001	471	100	85	93
ECV (%)	10 ± 2	19 ± 7	< 0.001	0.94	< 0.001	12	95	80	80
λ (%)	18 ± 3	31 ± 10	< 0.001	0.94	< 0.001	20	95	85	90
EHF (%)	25 ± 3	44 ± 12	< 0.001	0.95	< 0.001	32	84	100	92
ΔT1 (%)	39 ± 6	60 ± 9	< 0.001	0.97	< 0.001	50	95	95	95
T2 (ms)	40 ± 3	45 ± 10	0.114	0.67	0.070	45	40	95	68
Myocardium per slice-based approach									
T1 native (ms)	963 ± 27	1021 ± 44	< 0.001	0.89	< 0.001	980	90	75	83
T1 contrast 15 min (ms)	373 ± 56	318 ± 57	0.004	0.76	0.005	326	60	90	75
ECV (%)	22 ± 3	24 ± 5	0.383	0.58	0.372	21	80	45	63
λ (%)	39 ± 5	40 ± 9	0.925	0.51	0.914	41	80	35	35
EHF (%)	44 ± 4	52 ± 7	< 0.001	0.82	< 0.001	48	65	85	75
ΔT1 (%)	61 ± 6	69 ± 7	0.001	0.80	0.001	68	60	95	78
T2 (ms)	47 ± 2	52 ± 3	< 0.001	0.89	< 0.001	50	75	95	85
Myocardium per pixel-based approach									
T1 native (ms)	965 ± 25	1017 ± 43	< 0.001	0.85	< 0.001	984	75	80	78
T1 contrast, 15 min (ms)	379 ± 54	326 ± 54	0.004	0.77	0.004	328	60	90	75
ECV (%)	22 ± 3	23 ± 3	0.086	0.66	0.083	22	75	65	68
λ (%)	38 ± 5	38 ± 5	0.678	0.54	0.665	38	55	60	60
EHF (%)	44 ± 3	51 ± 7	< 0.001	0.82	< 0.001	47	70	80	78
ΔT1 (%)	61 ± 6	68 ± 6	0.001	0.79	0.002	68	60	95	78
T2 (ms)	48 ± 2	52 ± 3	< 0.001	0.88	< 0.001	50	80	95	88

Values are mean ± SD. The first *p* values represent comparison between controls and IIM using the Mann-Whitney *U* test, while the second *p* values represent the ROC analysis. Cutoffs were defined using Youden's index

IIM, idiopathic inflammatory myopathy; *ECV*, extracellular volume fraction; λ , partition coefficient; *EHF*, enhancement fraction; *ROC*, receiver operating characteristics; *AUC*, area under the curve

42 ms), while differences for native T1 were slightly higher (818–901 ms).

There was no significant difference of the myocardial T1 and T2 values between LGE-negative and LGE-positive patients (native T1 1014 ms vs. 1019 ms; $p = 0.846$, post contrast T1 319 ms vs. 330 ms; $p = 0.697$, T2 52 ms vs. 52 ms; $p = 0.927$). The skeletal muscle native T1 was tendentially slightly increased (919 ms vs. 990 ms; $p = 0.281$) and post contrast T1 decreased (387 ms vs. 367 ms; $p = 0.477$) in LGE-positive patients compared to LGE-negative patients, without reaching statistical significance. Skeletal muscle T2 was not significantly different between LGE-positive and LGE-negative patients (45 ms vs. 46 ms, $p = 0.859$).

Discussion

This study shows that MR relaxometry parameters are useful to accurately differentiate IIM patients from healthy controls in

myocardial and skeletal muscles, albeit not interchangeable. Since these parameters represent a summation of different tissue components in one region of interest, the varying percentages of such components depending on tissue type and disease should be taken into consideration. In this study, normal myocardium showed higher native T1 and lower post contrast T1 compared to normal skeletal muscles, which is consistent with other T1 mapping studies [21]. This can be explained by different proportions of intracellular and extracellular space (ECS) in myocardium and skeletal muscle. According to a study by Cieslar et al using ^{14}C -Inulin, in vivo ECS occupies 26.4% of total rat heart wet tissue weight (composed of 18.8% interstitial and 7.7% intravascular ECS) and 16.3% of rat skeletal muscle total wet tissue weight (composed of 14.5% interstitial and 1.8% intravascular ECS) [22]. Even if a direct comparison between human and rat hearts is not possible, these data suggest that interstitial and predominantly intravascular ECS are larger in the myocardium than in skeletal muscle. This is confirmed by a 30× higher myocardial perfusion,

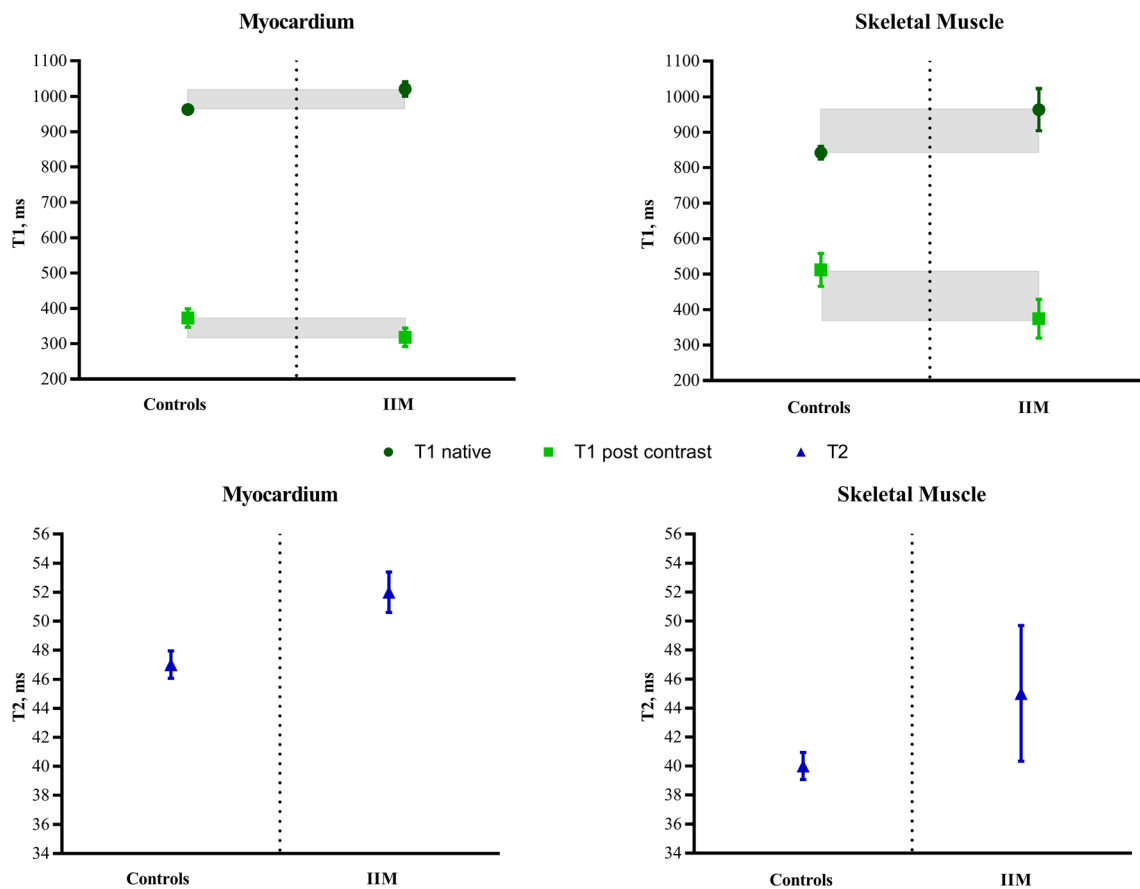


Fig. 1 Illustration of differences between T1 and T2 values in controls and IIM patients, as measured in the myocardium and skeletal muscle using the slice-based approach. Error bars indicate 95% confidence intervals. Gray areas illustrate the magnitude of the difference of native

and post contrast T1 between controls and IIM patients, with larger differences of T1 shortening after contrast injection between controls and IIM patients in skeletal muscles compared with the myocardium. IIM, idiopathic inflammatory myopathy

estimated at 95 ± 90 ml/min/100 g in the myocardium [23], compared with 3.1 ± 1.55 ml/min/100 g using $H_2^{15}O$ PET [24]. Since ECS is larger in the myocardium compared with skeletal muscle, it allows for higher gadolinium distribution in equilibrium phase as schematically illustrated in Fig. 2.

The best parameters to differentiate myocardial inflammation in IIM patients from normal myocardium in healthy controls were native T1 and T2, which is consistent with previous reports in acute viral myocarditis [15]. Post contrast T1 and T1-derived parameters (EHF, $\Delta T1$, and especially ECV) on the other hand were less discriminant in the myocardium. In contrast, post contrast T1 and T1-derived parameters were the best discriminating parameters in skeletal muscles. This may be explained by a lower baseline ECS of skeletal muscles [22] and thus higher sensitivity to increased gadolinium deposition due to pathologic ECS expansion in IIM patients. Indeed, in the myocardium, post contrast T1 shortening related to diffuse inflammation or fibrosis might be partially masked because of its relatively small magnitude compared with physiological T1 shortening due to higher baseline ECS, as illustrated in Fig. 1. Post contrast T1 and T1-derived parameters (EHF, $\Delta T1$, and especially ECV) were less discriminant in the

myocardium. In contrast, post contrast T1 and T-derived parameters were the best discriminating parameters in skeletal muscles. This may be explained by a lower baseline ECS of skeletal muscles [22] and thus higher sensitivity to increased gadolinium deposition due to pathologic ECS expansion in IIM patients. Indeed, in the myocardium, post contrast T1 shortening related to diffuse inflammation might be partially masked because of its relatively small magnitude compared with physiological T1 shortening due to higher baseline ECS, as illustrated in Fig. 1. The lower diagnostic performance of native T1 and T2 in skeletal muscles may be explained by several factors including the possible presence of different stages of fatty degeneration. This process is well known and described in skeletal muscle MRI of the limbs in chronic myositis patients [25]. T1 and T2 values may show important variation depending on the degree of fatty muscle degeneration, while post contrast T1 and T1-derived parameters reflecting T1 shortening seem to be less sensitive to such potential confounders. This might also explain the fact that there were no significant differences between T1-derived parameters of IIM subgroups, while patients with anti-synthetase syndrome showed slightly higher native T1, and patients with

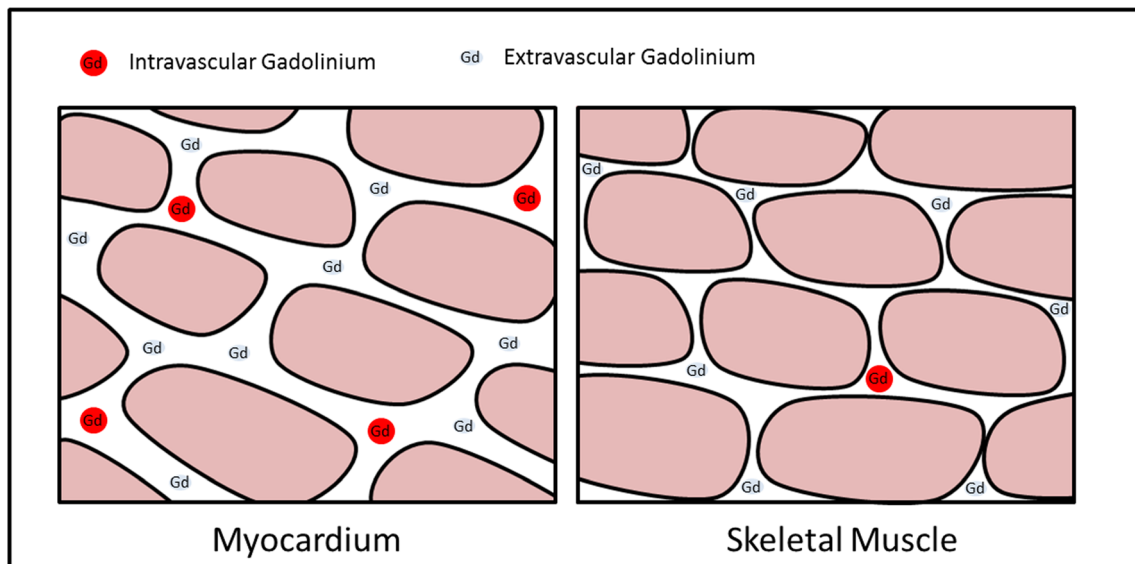


Fig. 2 Schematic illustration of different amounts of gadolinium in ECS during equilibrium phase based on the *in vivo* estimation of ECS composition in rats by Cieslar et al [22] with 4× higher amounts of intravascular gadolinium in myocardium as compared to skeletal muscle. ECS, extracellular space

polymyositis, dermatomyositis, and overlap syndrome showed slightly higher native T2. However, due to the small numbers of patients in the IIM subgroups and *p* values of 0.02–0.04, results of this subgroup analysis should not be overinterpreted.

There were no significant differences whether the myocardial T1 and T2 relaxation times were calculated on a per pixel (motion sensitive) or a per slice-based approach (less motion sensitive), measuring each inversion time (TI) on the whole myocardial slice then performing the exponential fit directly with these mean TI values. We therefore conclude that our methods were appropriate for segmentation, motion correction, and exclusion of extracardiac fat and cavity. The same holds true for the skeletal muscle analysis using a per slice-based approach, where just small differences of T1/T2 values and derived parameters in different muscles occurred, indicating a good performance of motion correction and exclusion of intramuscular tendons and perimascular fat.

As already discussed, all T1-derived parameters showed excellent diagnostic performance in skeletal muscles, clearly driven by post contrast T1. However, in the myocardium, ECV and λ were clearly less discriminant than EHF, $\Delta T1$, and post contrast T1. We believe that this can be explained by the non-linear nature of the ECV- and λ -equation. Substantial differences in native T1 and T1 shortening after gadolinium injection are strongly reduced by their inversion ($1/T1$). In addition, uncertainty of T1 measurements will be amplified by the complex ECV formula. EHF and $\Delta T1$, thanks to their simplified formula, might be less subject to these inversion and uncertainty issues. EHF and $\Delta T1$ may thus represent alternative measures for clinical routine, especially in highly vascularized tissues such as the myocardium, but also for example in the liver, spleen, or kidneys.

Nevertheless, ECV is a physiologically meaningful parameter to estimate ECS, while EHF and $\Delta T1$ are simplified surrogates. ECV was shown to reflect differences in tissue characteristics from different organs [26] and to correlate well with ECS volume expansion in several diseases [14, 27, 28]. However, interpretation of ECV as an absolute quantitative value representing true ECS volume might be misleading for several reasons. First, the intravascular pool is neglected in the ECV formula, although it can significantly influence these measurements in highly vascularized organs such as the myocardium, thus reducing sensitivity to detect small changes of interstitial ECS. This is even more complicated, as vascular ECS might be altered in patients with IIM, since IIM might include small vessels disease and vasodilatory properties may be impaired, in addition to fibrosis and inflammation in interstitial ECS [19]. Second, even if gadolinium is limited to the ECS, there is a rapid exchange of intra and extracellular water protons with a possible T1 shortening effect in the intracellular space as well [29]. Third, T1 post contrast values also depend on type, concentration, and timing of the gadolinium-based contrast media injection. However, the same is true for EHF and $\Delta T1$, which should be understood as relative parameters reflecting ECS fraction rather than representing absolute ECS.

Interestingly, only 4 out of 20 IIM patients showed definitely reduced EF < 50%, while all 20 controls showed normal EF. However, the fact that 16 out of 20 IIM patients showed normal EF highlights the importance of new non-invasive imaging biomarkers to detect subclinical myocardial involvement in IIM. Similar results have been published in patients with classic acute viral myocarditis (AVM), who often have normal systolic function. Kostakou et al [30] showed significantly lower longitudinal global strain based on echocardiographic speckle tracking in patients with AVM and normal global

systolic function compared to healthy controls, as there was no significant difference in LVEF between the two groups. Even if AVM and IIM with myocardial involvement are not directly comparable due to different pathophysiology of the disease, there might be also diastolic involvement in patients with IIM which should be investigated in future research projects.

There are limitations of this study. Clinical implications for T1 mapping in the myocardium as sole indicator may be limited due to overlap of the measured values between healthy controls and patients with IIM and cardiac involvement and site-related variability. However, cardiac involvement in IIM is often subclinical and combined analysis of myocardial native T1, T1-derived parameters, and T2 might have an incremental clinical value in IIM patients undergoing cardiac MR imaging, especially when combined with skeletal muscle T1 and T2 mapping analysis when compared to site-specific normal values. Comparison of different muscle types is complicated, since there are many possible confounding factors such as intramuscular tendons in skeletal muscles and moving artifacts in the myocardium. However, intramuscular tendons and perimuscular fat in skeletal muscles and endocavitary blood and pericardial fat in the myocardium have been carefully excluded from the measurements. Skeletal muscle and myocardial segmentation were manually corrected on each TI image. In addition, similar results in the per slice-based and the per pixel-based approach for the myocardium and small differences of the measured mapping parameters between different skeletal muscles indicate that these confounders have been successfully minimized. Another limitation is the relatively small patient population owed to the difficulty to recruit IIM patients with cardiac inflammation, elevated troponins and contemporary cardiac MR imaging. Nevertheless, differences were highly significant. A more clinically oriented, larger study in IIM patients should prospectively investigate the utility of MR relaxometry to analyze longitudinal myocardial and skeletal remodeling under treatment. Furthermore, EHF and $\Delta T1$ should be compared to ECV in different pathologies other than myocarditis, as well as in other organs.

MR relaxometry showed excellent performance to differentiate IIM patients from healthy controls in the myocardium as well as in skeletal muscle. However, different tissue characteristics should be taken into consideration when interpreting T1 and T2 relaxation times, as well as their derived parameters. Native T1 and T2 were the best discriminating parameters in the myocardium, while they were less discriminant in skeletal muscles, probably due to the different degrees of fatty muscle degeneration in chronic myositis. In contrast, T1 post contrast, $\Delta T1$, EHF, and especially ECV were less sensitive to extracellular volume expansion in the highly vascularized myocardium compared to the less vascularized skeletal muscles. Due to the complexity of the ECV formula, $\Delta T1$ and EHF might be considered as simplified alternatives in highly vascularized tissues.

Acknowledgements AH received a research grant from the Helmut-Hartweg-Foundation of the Swiss Academy of Medical Sciences (SAMS). JL received a research grant from the Institute of Cardiometabolism and Nutrition (ICAN). The project was financially supported by the Institut Universitaire d'Ingénierie en Santé (IUIS).

We thank Dr. Alain Giron for his statistical advice for this manuscript.

Funding This study has received funding by the Helmut-Hartweg-Foundation of the Swiss Academy of Medical Sciences (SAMS), the Institute of Cardiometabolism and Nutrition (ICAN), and by the Institut Universitaire d'Ingénierie en Santé (IUIS). Paris, France.

Compliance with ethical standards

Guarantor The scientific guarantor of this publication is Dr. Nadjia Kachenoura.

Conflict of interest The authors of this manuscript declare no relationships with any companies whose products or services may be related to the subject matter of the article.

Statistics and biometry Dr. Alain Giron kindly provided statistical advice for this manuscript.

Informed consent Written informed consent was obtained from all subjects (patients) in this study.

Ethical approval Institutional Review Board approval was obtained.

Study subjects or cohorts overlap The data presented in this paper are novel and have never been published before. Since idiopathic inflammatory myositis (IIM) with myocardial involvement is a very rare condition and a valuable model of myocardial and skeletal muscle alterations, we used the same IIM patients in the present manuscript than those previously used in the JCMR paper entitled "Non-invasive differentiation of idiopathic inflammatory myopathy with cardiac involvement from acute viral myocarditis using cardiovascular magnetic resonance imaging T1 and T2 mapping". 20.1 (2018): 11. However, while the JCMR paper focused on the usefulness of skeletal muscles conventional T1 and T2 mapping indices in differentiating acute viral myocarditis (AVM) from IIM, the present paper focusses on the comparison of several established and newly proposed myocardial and skeletal muscle mapping-derived biomarkers in terms of their ability to distinguish IIM patients from controls. There are no AVM patients in this paper, so we present a different patient population.

Methodology

- retrospective
- case-control study
- performed at one institution

Publisher's note Springer Nature remains neutral with regard to jurisdictional claims in published maps and institutional affiliations.

References

1. Hamlin SA, Henry TS, Little BP, Lerakis S, Stillman AE (2014) Mapping the future of cardiac MR imaging: case-based review of T1 and T2 mapping techniques. *Radiographics* 34:1594–1611. <https://doi.org/10.1148/rg.346140030>

2. Schelbert EB, Messroghli DR (2016) State of the art: clinical applications of cardiac T1 mapping. *Radiology* 278:658–676. <https://doi.org/10.1148/radiol.2016141802>
3. Messroghli DR, Radjenovic A, Kozerke S, Higgins DM, Sivanathan MU, Ridgway JP (2004) Modified look-locker inversion recovery (MOLLI) for high-resolution T1 mapping of the heart. *Magn Reson Med* 52:141–146. <https://doi.org/10.1002/mrm.20110>
4. Roujol S, Weingärtner S, Foppa M et al (2014) Accuracy, precision, and reproducibility of four T1 mapping sequences: a head-to-head comparison of MOLLI, ShMOLLI, SASHA, and SAPPHIRE. *Radiology* 272:683–689. <https://doi.org/10.1148/radiol.14140296>
5. Thavendiranathan P, Walls M, Giri S et al (2012) Improved detection of myocardial involvement in acute inflammatory cardiomyopathies using T2 mapping. *Circ Cardiovasc Imaging* 5:102–110. <https://doi.org/10.1161/CIRCIMAGING.111.967836>
6. Bellin MF, Van Der Molen AJ (2008) Extracellular gadolinium-based contrast media: an overview. *Eur J Radiol* 66:160–167. <https://doi.org/10.1016/j.ejrad.2008.01.023>
7. Strich G, Hagan PL, Gerber KH, Slutsky RA (1985) Tissue distribution and magnetic resonance spin lattice relaxation effects of gadolinium-DTPA. *Radiology* 154:723–726. <https://doi.org/10.1148/radiology.154.3.3969477>
8. Sueyoshi E, Sakamoto I, Uetani M (2009) Myocardial delayed contrast-enhanced MRI: relationships between various enhancing patterns and myocardial diseases. *Br J Radiol* 82:691–697. <https://doi.org/10.1259/bjtr/23291589>
9. Kellman P, Wilson JR, Xue H, Ugander M, Arai AE (2012) Extracellular volume fraction mapping in the myocardium, part 1: evaluation of an automated method. *J Cardiovasc Magn Reson* 14: 63
10. Jerosch-Herold M, Sheridan DC, Kushner JD et al (2008) Cardiac magnetic resonance imaging of myocardial contrast uptake and blood flow in patients affected with idiopathic or familial dilated cardiomyopathy. *Am J Physiol Heart Circ Physiol* 295:H1234–H1242. <https://doi.org/10.1152/ajpheart.00429.2008>
11. Yoon JH, Lee JM, Paek M, Han JK, Choi BI (2016) Quantitative assessment of hepatic function: modified look-locker inversion recovery (MOLLI) sequence for T1 mapping on Gd-EOB-DTPA-enhanced liver MR imaging. *Eur Radiol* 26:1775–1782. <https://doi.org/10.1007/s00330-015-3994-7>
12. Besa C, Bane O, Jajamovich G, Marchione J, Taouli B (2015) 3D T1 relaxometry pre and post gadoxetic acid injection for the assessment of liver cirrhosis and liver function. *Magn Reson Imaging* 33: 1075–1082. <https://doi.org/10.1016/j.mri.2015.06.013>
13. Haaf P, Garg P, Messroghli DR, Broadbent DA, Greenwood JP, Plein S (2016) Cardiac T1 mapping and extracellular volume (ECV) in clinical practice: a comprehensive review. *J Cardiovasc Magn Reson* 18:89. <https://doi.org/10.1186/s12968-016-0308-4>
14. Miller CA, Naish JH, Bishop P et al (2013) Comprehensive validation of cardiovascular magnetic resonance techniques for the assessment of myocardial extracellular volume. *Circ Cardiovasc Imaging* 6:373–383. <https://doi.org/10.1161/CIRCIMAGING.112.000192>
15. Lurz P, Luecke C, Eitel I et al (2016) Comprehensive cardiac magnetic resonance imaging in patients with suspected myocarditis: the MyoRacer-Trial. *J Am Coll Cardiol* 67:1800–1811. <https://doi.org/10.1016/j.jacc.2016.02.013>
16. Ferreira VM, Piechnik SK, Dall'Armellina E et al (2013) T1 mapping for the diagnosis of acute myocarditis using CMR: comparison to T2-weighted and late gadolinium enhanced imaging. *JACC Cardiovasc Imaging* 6:1048–1058
17. Puntmann VO, Carr-White G, Jabbour A et al (2016) T1-mapping and outcome in nonischemic cardiomyopathy. *JACC Cardiovasc Imaging* 9:40–50. <https://doi.org/10.1016/j.jcmg.2015.12.001>
18. Gupta R, Wayangankar SA, Targoff IN, Hennebry TA (2011) Clinical cardiac involvement in idiopathic inflammatory myopathies: a systematic review. *Int J Cardiol* 148:261–270. <https://doi.org/10.1016/j.ijcard.2010.08.013>
19. Schwartz T, Diederichsen LP, Lundberg IE, Sjaastad I, Sanner H (2016) Cardiac involvement in adult and juvenile idiopathic inflammatory myopathies. *RMD Open* 2:e000291. <https://doi.org/10.1136/rmdopen-2016-000291>
20. Huber AT, Bravetti M, Lamy J et al (2018) Non-invasive differentiation of idiopathic inflammatory myopathy with cardiac involvement from acute viral myocarditis using cardiovascular magnetic resonance imaging T1 and T2 mapping. *J Cardiovasc Magn Reson* 20:11. <https://doi.org/10.1186/s12968-018-0430-6>
21. Barison A, Gargani L, De Marchi D et al (2015) Early myocardial and skeletal muscle interstitial remodelling in systemic sclerosis: insights from extracellular volume quantification using cardiovascular magnetic resonance. *Eur Heart J Cardiovasc Imaging* 16:74–80. <https://doi.org/10.1093/ehjci/jeu167>
22. Cieslar J, Huang MT, Dobson GP (1998) Tissue spaces in rat heart, liver, and skeletal muscle in vivo. *Am J Physiol* 275:R1530–R1536
23. Iida H, Kanno I, Takahashi A et al (1988) Measurement of absolute myocardial blood flow with H215O and dynamic positron-emission tomography. Strategy for quantification in relation to the partial-volume effect. *Circulation* 78:104–115. <https://doi.org/10.1161/01.CIR.78.1.104>
24. Ruotsalainen U, Raitakari M, Nuutila P et al (1997) Quantitative blood flow measurement of skeletal muscle using oxygen-15-water and PET. *J Nucl Med* 38:314–319
25. Day J, Patel S, Limaye V (2017) The role of magnetic resonance imaging techniques in evaluation and management of the idiopathic inflammatory myopathies. *Semin Arthritis Rheum* 46:642–649. <https://doi.org/10.1016/j.semarthrit.2016.11.001>
26. Bandula S, Banyersad SM, Sado D et al (2013) Measurement of tissue interstitial volume in healthy patients and those with amyloidosis with equilibrium contrast-enhanced MR imaging. *Radiology* 268:858–864. <https://doi.org/10.1148/radiol.13121889>
27. Sado DM, Flett AS, Banyersad SM et al (2012) Cardiovascular magnetic resonance measurement of myocardial extracellular volume in health and disease. *Heart* 98:1436–1441. <https://doi.org/10.1136/heartjnl-2012-302346>
28. Fontana M, White SK, Banyersad SM et al (2012) Comparison of T1 mapping techniques for ECV quantification. Histological validation and reproducibility of ShMOLLI versus multibreath-hold T1 quantification equilibrium contrast CMR. *J Cardiovasc Magn Reson* 14:88. <https://doi.org/10.1186/1532-429X-14-88>
29. Koenig SH, Spiller M, Brown RD 3rd, Wolf GL (1986) Relaxation of water protons in the intra- and extracellular regions of blood containing Gd (DTPA). *Magn Reson Med* 3:791–795. <https://doi.org/10.1002/mrm.1910030514>
30. Kostakou PM, Kostopoulos VS, Tryfou ES et al (2018) Subclinical left ventricular dysfunction and correlation with regional strain analysis in myocarditis with normal ejection fraction. A new diagnostic criterion. *Int J Cardiol* 259:116–121. <https://doi.org/10.1016/j.ijcard.2018.01.058>